Purification and Characterization of Two Polymorphic Variants of Short Chain Acyl-CoA Dehydrogenase Reveal Reduction of Catalytic Activity and Stability of the Gly185Ser Enzyme†

Tien V. Nguyen,‡ Charles Riggs,§ Dusica Babovic-Vuksanovic,‡ Yong-Sung Kim,|| John F. Carpenter,|| Thomas P. Burghardt,⊥ Niels Gregersen,@ and Jerry Vockley*,‡

Department of Medical Genetics, Mayo Clinic and Foundation, Rochester, Minnesota 55905, Human Performance Laboratory, University of Arkansas, Fayetteville, Arkansas 72701, Department of Pharmaceutical Sciences, University of Colorado Health Science Center, Denver, Colorado 80262, Department of Biochemistry and Molecular Biology, Mayo Clinic and Foundation, Rochester, Minnesota 55905, and Research Unit for Molecular Medicine, Aarhus University Hospital and Faculty of Health Sciences, Skejby Sygehus, Aarhus, Denmark

Received April 26, 2002; Revised Manuscript Received July 10, 2002

ABSTRACT: Short chain acyl-CoA dehydrogenase (SCAD) is a homotetrameric flavoenzyme that catalyzes the first intramitochondrial step in the β-oxidation of fatty acids. Two polymorphisms in the coding region of the SCAD gene, 511C>T (R147W) and 625G>A (G185S), have been shown to be associated with an increased level of ethylmalonic acid excretion in urine, a clinical characteristic of SCAD deficiency. To characterize the biochemical consequences of these variations, in vitro site-directed mutagenesis and prokaryotic expression were used to produce the corresponding SCAD variant proteins. Both variant proteins were unstable when produced in *Escherichia coli*, but could be rescued and subsequently purified by coexpressing them with the bacterial chaperonin GroEL/ES. The k_{cat}/K_m values of the green wild-type, R147W, and G185S SCAD enzymes coexpressed with GroEL/ES were 33, 30, and 10 μM^{-1} s^{-1}, respectively. There were minimal differences in the kinetic parameters measured for the green, degreened, and wild-type enzymes coexpressed with GroEL/ES, and the R147W variant when butyryl-CoA was used as a substrate. The catalytic efficiency of the G185S variant enzyme, however, was reduced compared to that of the wild-type enzyme. The thermal and guanidine HCl stability of the purified enzymes as determined by fluorescence, far-UV CD spectroscopy, and incubation-induced rest activity showed the following order of relative stability: wild-type enzyme > R147W > G185S. Near-UV CD spectroscopy indicated that these impairments are caused by decreased flexibility in the tertiary conformation of the two mutant enzymes. The common SCAD polymorphisms may lead to clinically relevant alterations in enzyme function.

Short chain acyl-CoA dehydrogenase (EC 1.3.99.2, SCAD)[1] is a member of the highly conserved acyl-CoA dehydrogenase (ACD) family, which is made up of mitochondrial flavoenzymes containing one molecule of FAD per subunit (*1*−*7*). Four members of this family catalyze the first intramitochondrial step in the α,β-dehydrogenation of fatty acyl-CoAs with maximum activity for various chain length substrates. The X-ray crystal structures for several ACDs, including SCAD, have been determined (*8*−*12*). Native SCAD is a homotetramer with a molecular mass of 168 kDa and contains one FAD prosthetic group per subunit. In humans, the deficiency of an ACD can lead to considerable morbidity and mortality in both children and adults (*13*, *14*). Laboratory diagnosis of these disorders is often difficult. This has been particularly true for SCAD. Excretion of ethylmalonic acid (EMA) in the urine is considered the hallmark of SCAD deficiency, but is nonspecific and has been reported in a variety of clinical settings (*15*−*20*). Two nucleotide variations have been identified in the coding region of the SCAD gene that lead to amino acid substitutions in the mature enzyme: 511C>T (R147W) and 625G>A (G185S). These two variations are present either in homozygous form or as a compound heterozygote for one of each allele at a frequency of 14% in the general population, as compared to 69% in a group of 133 patients with a variety of neurologic conditions and increased levels of EMA excretion in urine (*21*). The G185S and R147W variant SCADs in crude extracts from tissue culture cells expressing these alleles are

† This work was supported by NIH Grant DK54936, a grant from the March of Dimes to J.V., and the Danish Center for Human Genome Research, Danish Research Council, Institute of Experimental Clinical Research, Aarhus County Research Initiative, to N.G.

* To whom correspondence should be addressed.
‡ Department of Medical Genetics, Mayo Clinic and Foundation.
§ University of Arkansas.
|| University of Colorado Health Science Center.
⊥ Department of Biochemistry and Molecular Biology, Mayo Clinic and Foundation.
@ Aarhus University Hospital and Faculty of Health Sciences.

[1] Abbreviations: AACoA, acetoacetylcoenzyme A; ACD, acylcoenzyme A dehydrogenase; BCAD, branched chain acylcoenzyme A dehydrogenase; CCoA, crotonoylcoenzyme A; CD, circular dichroism; CoA, coenzyme A; C4CoA, butyrylcoenzyme A; EDTA, ethylenediaminetetraacetic acid; EFAD, enzyme containing FAD; EMA, ethylmalonic acid; ETF, electron-transferring flavoprotein; FAD, flavin adenine dinucleotide; GdnHCl, guanidine hydrochloride; HPLC, high-performance liquid chromatography; MCAD, medium chain acylcoenzyme A dehydrogenase; PCR, polymerase chain reaction; SCAD, short chain acylcoenzyme A dehydrogenase; SD, standard deviation; WT, wild type; WTGR, wild type coexpressed with chaperonin GroEL/ES.

10.1021/bi026030r CCC: $22.00
Published on Web 08/21/2002

less stable and more thermolabile than the wild-type enzyme, raising the possibility that the variant enzymes may play a role in the development of clinical disease (*21*). To further investigate this, the variant enzymes were produced in a prokaryotic expression system, and the biophysical and enzymatic properties of purified wild-type and variant SCADs were determined.

MATERIALS AND METHODS

Construction of SCAD Expression Plasmids. For expression experiments, the wild-type SCAD cDNA was inserted into the prokaryotic expression vector pKK 223-3 (Pharmacia, Piscataway, NJ; pKhSCAD). Initial experiments indicated that the level of SCAD expression in this system was too low to allow easy purification, so the first 111 nucleotides of the coding insert of the mature protein form were altered via PCR mutagenesis to reflect *Escherichia coli* codon bias usage without altering the amino acid sequence of the enzyme (*22*) (5′-^{1}ATG **C**T**G** CAC ACC ATC TAC CAG TCT GT**T** GAA CTG CC**G** GA**A** AC**T** CAC CAG ATG **C**TG CT**G** CAG AC**T** TGC CG**C** GAC TT**C** GC**T** GA**A** AA**A** GA**A** **C**TG TT**C** CC**G** AT**C** GCA GC**T** CAG GT**T**^{111}-3′). Altered nucleotides are bold and underlined.

Polymerase chain reaction (PCR) site-directed mutagenesis was employed to construct the variant SCAD cDNA sequences. All mutagenic primers were synthesized by the Molecular Biology Core Facility at the Mayo Clinic and Foundation. For the 511C>T variation, the upstream PCR primer was 5′-CGT GCC ACC ACC GCC **TGG** GCC GAG GGC G-3′, and for the 625G>A variation, it was 5′-GAC AGA GCC CTG CAA AAC AAG **AGC** ATC AGT GCC TTC CTG GTC-3′. PCR was performed with cycling conditions of 60 °C annealing, 72 °C extension, and 94 °C denaturing for 35 cycles, using PCR SuperMix with *Taq* polymerase (Gibco BRL, Rockville, MD). PCR products were digested with *Apa*I (Boehringer Mannheim, Mannheim, Germany) and *Bgl*II (Gibco BRL) and inserted into the same position in the wild-type vector. All sequences were confirmed with automated DNA sequencing.

Expression and Purification of SCADs in E. coli Cells with and without Coexpression of the Chaperonin GroEL/ES. pKhSCAD and a plasmid containing the genes for the bacterial chaperonins GroEL and GroES (pGroEL/ES) (*23*−*27*) were introduced into *E. coli* host strain XL1 Blue (Strategene, La Jolla, CA) and maintained under appropriate selective conditions for each plasmid. Large-scale production of SCADs was performed essentially as described previously (*28*−*30*). The cells were harvested after induction for 4 h with IPTG. SCAD was purified from cell free extracts by chromatography on DEAE-Sepharose Fast Flow, fractionation with 45−65% ammonium sulfate, and chromatography on 10 μm ceramic hydroxyapatite column as described previously (*28*−*30*). The purity of the pooled enzyme fractions from this column was judged by SDS−polyacrylamide gel electrophoresis (*31*).

Removal of the CoA Persulfide Ligand of SCAD Preparations. SCAD and other ACDs produced in bacterial expression systems exhibit a green color due to a CoA persulfide bound to the enzyme (*32*−*34*). To remove this, the concentrated final SCAD fractions were reduced by anaerobic dialysis versus 50 mM potassium phosphate, 1 mM EDTA (pH 7.4), and 5 mM sodium hydrosulfite for 2 h. The reduced ("degreened") enzyme solution was then applied to a Thiopropyl Sepharose-6B column, incubated for 20 min, and eluted with 50 mM potassium phosphate, 1 mM EDTA, and 0.1 M KCl (pH 7.4). Enzyme-containing fractions were pooled and dialyzed against 50 mM potassium phosphate and 1 mM EDTA (pH 7.4). Glycerol was added to 30% for storage at −20 °C. Protein concentrations were determined using the DC assay system from Bio-Rad (Hercules, CA).

Enzyme and Spectral Assays. The ferricenium hexafluorophosphate reduction assay was performed as described using a Beckman (Fullerton, CA) DU 7400 spectrophotometer (*2*, *35*). The anaerobic electron transferring flavoprotein (ETF) reduction assay was performed using an LS50B fluorescence spectrophotometer from Perkin-Elmer (Norwalk, CT) with a heated cuvette block set to 32 °C as described previously (*28*−*30*, *36*). The software program *UltraFit* version 3.02 (Biosoft, Cambridge, England) on a Macintosh personal computer was used to fit the data to the Michaelis−Menten equation using nonlinear regression analysis with robust weighting. The mean and 95% confidence interval are reported for each parameter. For temperature and pH stability studies, a sample of the purified enzyme was diluted to a final concentration of 30−50 milliunits/mL at the indicated pH and temperature, and incubated for 5 h prior to the assay with the ferricenium hexafluorophosphate. Formation of the charge transfer complex after addition of the substrate was monitored by observing the decrease in absorbance in the 445 nm region and the appearance of the long-wavelength band at 580 nm as described previously (*28*, *37*−*39*). Spectral scans were performed using a Beckman (Palo Alto, CA) DU7400 spectrophotometer equipped with a computer. Briefly, 400 μL of a 0.97−2.44 μM SCAD sample diluted in 10 mM potassium phosphate (pH 7.0) was placed in a quartz cuvette with a round top at room temperature. The cuvette was then sealed with a rubber stopper, and using a needle, 10 alternating cycles of vacuum and argon were applied to remove molecular oxygen. Butyryl-CoA was added in sequential amounts using a 50 μL Hamilton syringe attached to an automatic dispenser. Butyryl-CoA concentrations varied from 0 to 17 μM. The reaction reached equilibrium within a few seconds after each substrate addition; no further change in the spectra was recognized on additional repeated scans.

Near-UV, far-UV, and visible CD spectra were recorded in a 2 mm path length cuvette at 20 °C on a Jasco (Easton, MD) J-715 spectrometer. The enzyme was diluted with 10 mM Tris (pH 7.0) to a concentration of 5 μM for near-UV and visible spectra and 0.38−0.57 μM for the far-UV range after removal of molecular oxygen (*28*, *37*−*39*). To obtain CD spectra of enzyme−substrate complexes, 1 mM (or 25 μM) butyryl-CoA or acetoacetyl-CoA solution was added to the diluted enzyme to give the desired substrate concentration, and measurements were taken over wavelength ranges of 180−260 and 250−700 nm. After equilibrium had been reached (within a few seconds), an average spectrum from three scans was utilized for further calculations. Ellipticity (millidegrees) was measured at each wavelength $\{\Theta\}_{obs}$ and expressed as the mean residue molar ellipticity $\{\Theta\}$ (degrees-square centimeter per decimole), defined as $\{\Theta\} = \Theta_{obs}$-MRW/(10$lc$), where Θ_{obs} is the observed ellipticity in degrees, c is the protein concentration in grams per milliliter,

and l is the length of the light path in centimeters. A mean residue weight (MRW) of 108 is used for calculations. The near-UV CD titration data were fit to the equation

$$Y(x) = Y_o + a(1 - e^{-bx}) \quad (1)$$

where Y is defined as the molar ellipticity when $x \geq 0$, Y_o is the molar ellipticity of the enzyme without substrate, x is the molar ratio of the substrate to enzyme concentrations (equivalents), and a and b are the coefficients of the fitted equation, using Sigma Plot 2001 version 7.0 software. The maximal conformation change of SCAD upon interaction with substrate and nonsubstrate at specific wavelengths was determined by

$$\Delta\Theta_{max} = \lim_{x\to\infty} Y(\infty) - Y(0) = \lim_{x\to\infty} a(1 - e^{-bx}) = a \quad (2)$$

Thermal and Guanidine HCl (GdnHCl) Unfolding of SCADs As Determined by Fluorescence and CD. Fluorescence measurements were performed on an Aviv (Lakewood, NY) ATF 105 spectrofluorometer equipped with a constant-temperature cell holder. The protein concentration for all fluorescence measurements was 10 μg/mL (0.06 μM) in 10 mM Tris buffer (pH 7). To measure tryptophan fluorescence, excitation was at 295 nm and emission was recorded in the range of 400−300 nm with 4 and 8 nm bandwidths for excitation and emission, respectively. CD measurements were performed on an Aviv 62DS circular dichroism spectrometer (Aviv) between 190 and 260 nm with a 2 mm path length at a protein concentration of 80 μg/mL (0.48 μM) in 10 mM Tris buffer (pH 7). The baseline spectrum was subtracted from the sample spectrum. Each spectrum represents the average of three scans. Both fluorescence and far-UV CD spectroscopy were used to assess thermal and GdnHCl unfolding of the purified SCADs (*40*−*43*). Unfolding curves as a function of temperature were constructed by measuring intrinsic tryptophan fluorescence at an excitation wavelength of 295 nm and an emission wavelength of 340 nm with an increase in temperature from 20 to 85 °C every 0.5 °C with a scan rate of 0.75 °C/min. The far-UV CD spectrum was recorded at 222 nm from 20 to 85 °C every 1 °C with a scan rate of 1 °C/min. For substrate binding experiments, either excess substrate or a substrate:FAD molar ratio of 1:1 was used. For the GdnHCl unfolding assays, all tested samples were incubated at the same time overnight at room temperature, and at the given GdnHCl concentrations. Unfolding curves as a function of GdnHCl concentration were constructed by measuring intrinsic tryptophan fluorescence at an excitation wavelength of 295 nm and over an emission wavelength range of 370−330 nm to follow the maximum wavelength (λ_{max}). The far-UV CD spectrum was recorded at 222 nm.

Size-Exclusion High-Performance Liquid Chromatography (SE-HPLC). Wild-type and mutant SCADs were analyzed by SE-HPLC using a TOSOHAAS G2000SWXL size-exclusion column as described previously (*40*). Three micrograms of protein was injected.

Molecular Modeling of Variant SCAD Structures. The structure of wild-type human SCAD was modeled from the rat enzyme structure using the Insight II 2000 package of software from Molecular Simulations (San Diego, CA) and a Silicon Graphics (Mountain View, CA) O2 workstation as previously described (*28*). The "manual rotomer" option was used to optimize the position of atoms of the side chains of specific amino acid residues and examine the energy minima of the various possible conformations. The desired changes in amino acid structure were made using the homology module of Insight II, and the structures were energy-minimized (*28*).

Table 1: Effect of the GroEL/ES Coexpression on Specific Activity Level in Crude Cell Extracts of Wild-Type and Variant SCAD Enzymes Prior to Degreening As Determined by the Anaerobic ETF Fluorescence Reduction Assay with Butyryl-CoA at 50 μM

enzyme	coexpression with GroEL/ES	specific activity of crude extract (milliunits/mg of protein ± SD)[a]
WT	no	190 ± 3
	yes	1080 ± 30
R147W	no	18 ± 0.7
	yes	510 ± 60
G185S	no	80 ± 1
	yes	1100 ± 50

[a] The cells were harvested after induction for 4 h. Assays were performed in triplicate.

RESULTS AND DISCUSSION

The level of excretion of ethylmalonic acid in urine, a hallmark of SCAD deficiency, is increased in individuals who are homozygous for either of two polymorphisms in the SCAD gene encoding R147W and G185S variant proteins (or compound heterozygous for one of each allele). These variants have been identified in patients with a variety of neurologic and neuromuscular symptoms, but the clinical relevance of this is unclear. The current study directly examines the biochemical and enzymatic properties of purified recombinant wild-type and variant SCADs, and provides insight into the effects of the polymorphisms on their enzymatic function.

Overexpression of Wild-Type, R147W, and G185S SCADs in E. coli and Stabilization by the Chaperonin GroEL/ES. All expression experiments were performed with the codon bias vector. The specific activities of the crude cellular extracts of both R147W and G185S variant enzymes following induction were much lower than for the wild type (Table 1). Impairment of folding of the R147W and G185S variants of SCAD when overexpressed in *E. coli* was manifested by a tendency for the recombinant protein to form aggregates during induction. In addition, subsequent purification of the soluble recombinant enzyme was difficult, resulting in low yields and inactive enzyme. Coexpression with the bacterial chaperonin proteins GroEL/ES overcame this problem, increasing the amount of soluble enzyme protein as confirmed by Western blotting (data not shown) and specific activity in the cellular extract 5.6−28-fold (Table 1), with no change in the amount of mRNA in the induced cells (data not shown). This allowed efficient purification of the two variant enzymes.

Purification of SCAD Wild-Type and Variant Enzymes. Final enzyme preparations were at least 95% pure as judged by SDS−PAGE (data not shown). The substrate specificities of the purified wild-type and variant SCADs are shown in Table 2. Maximum specific activity of the final preparations was obtained with butyryl-CoA as a substrate (Table 2). Of note is the fact that the G185S variant exhibited a lower

Table 2: Specific Activity of Purified Wild-Type and Variant SCADs Measured Prior to Degreening with the Anaerobic ETF Fluorescence Reduction Assay Using a Variety of Substrates at the Tested Concentration of 50 μM

	specific activity for active substrates[b] (units/mg of protein ± SD)				
enzyme[a]	butyryl-CoA	hexanoyl-CoA	octanoyl-CoA	2-methylbutyryl-CoA	isobutyryl-CoA
wild type	5.9 ± 0.4	3.2 ± 0.1	0.06 ± 0.004	1.5 ± 0.3	0.03 ± 0.004
R147W	4.7 ± 0.1	3.7 ± 0.2	0.01 ± 0.006	2.5 ± 0.1	0.06 ± 0.06
G185S	2.9 ± 0.2	0.9 ± 0.03	0.009 ± 0.004	0.3 ± 0.1	0.20 ± 0.002

[a] Enzymes were purified after coexpression with GroEL/ES and prior to degreening. [b] Values represent means ± the standard deviation of at least three assays.

Table 3: Comparison of the Kinetic Parameters of Wild-Type SCAD without and with Reduction by Dithionite (Green and Degreened Forms) As Measured with the Anaerobic ETF Fluorescence Reduction Assay[a]

	green enzyme			degreened enzyme		
substrate	K_m (μM)	k_{cat} (s^{-1})	tetramer catalytic efficiency (μM^{-1} s^{-1})	K_m (μM)	k_{cat} (s^{-1})	tetramer catalytic efficiency (μM^{-1} s^{-1})
butyryl-CoA	0.38 ± 0.09 (N = 24)[b]	11 ± 1	28 ± 8	0.32 ± 0.05 (N = 27)	9.4 ± 0.3	29 ± 5
hexanoyl-CoA	4.4 ± 0.8 (N = 26)	10 ± 0.5	2.3 ± 0.5	5.3 ± 0.7 (N = 22)	7.2 ± 0.3	1.4 ± 0.2
octanoyl-CoA	15 ± 4 (N = 24)	0.33 ± 0.03	0.02 ± 0.01	17 ± 6 (N = 15)	0.25 ± 0.03	0.02 ± 0.01
2-methylbutyryl-CoA	19 ± 8 (N = 22)	6 ± 1	0.3 ± 0.2	40 ± 13 (N = 18)	10 ± 2	0.2 ± 0.1

[a] All values represent the standard deviation and 95% confidence intervals calculated as described in the text. Substrate concentrations were tested in the range of 0.1−50 μM. [b] N is the number of determinations.

Table 4: Kinetic Parameters of Wild-Type and Variant SCADs (Green Form) Measured with the Anaerobic ETF Fluorescence Reduction Assay and Butyryl-CoA as the Substrate[a]

enzyme[b]	K_m (μM)	k_{cat} (s^{-1})	tetramer catalytic efficiency[c] (μM^{-1} s^{-1})
WT	0.29 ± 0.06 (N = 25)[d]	9.6 ± 0.4	33 ± 8
R147W	0.45 ± 0.04 (N = 24)	13 ± 2	30 ± 7
G185S	0.75 ± 0.09 (N = 24)	7.7 ± 0.2	10 ± 2

[a] The substrate concentrations were tested in a range of 0.1−50 μM. [b] All enzymes were coexpressed with GroEL/ES. [c] All values represent the mean and 95% confidence intervals calculated as described in the text. [d] N is the number of determinations.

specific activity with butyryl-CoA as the substrate, and utilizes longer chain substrates less well than either the wild-type or R147W SCAD. The latter two enzymes have similar substrate specificities. All of the purified enzyme solutions were a light green color, suggesting the presence of a bound CoA persulfide molecule, as previously described for butyryl-CoA dehydrogenase (BCAD) from *Megasphaera elsdenii*, rat SCAD, and other ACDs (*10*, *32*−*34*, *44*). Concern about the effects on enzyme function of the bound CoA persulfide initially led us to attempt to remove it prior to further characterization of the purified enzymes. Removal of a bound CoA persulfide ligand from wild-type SCAD (degreening) was accomplished by anaerobic reduction with sodium hydrosulfite followed by chromatography on Thiopropyl-Sepharose 6B (*32*−*34*). Degreening or coexpression of wild-type SCAD with GroEL/ES only minimally altered the kinetic parameters of the purified wild-type enzyme measured with butyryl-CoA as a substrate (Tables 3 and 4). Since attempts to degreen the two variant SCADs led to loss of FAD and significantly reduced the stability (data not shown), unreduced enzyme preparations were used for further enzymatic characterization.

The G185S variant showed impaired kinetic parameters compared to those of the wild-type enzyme when measured with butyryl-CoA as the substrate and ETF as the final electron acceptor, while the K_m of the R147W variant was only slightly higher than that of wild-type SCAD (Table 4).

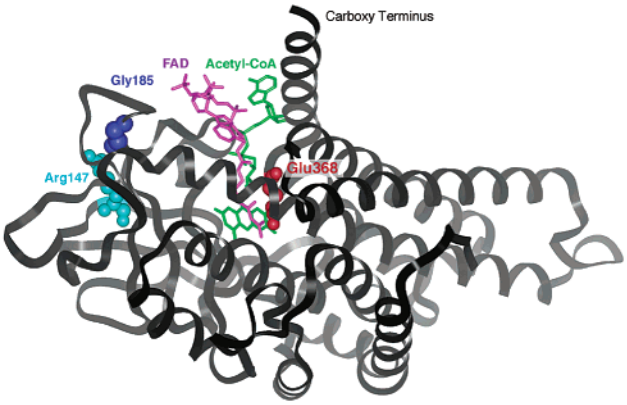

FIGURE 1: Molecular model of the structure of human SCAD and the polymorphic variants. The predicted positions of R147 and G185 in the modeled structure of human SCAD are shown. The primary carbon backbone of the enzyme is rendered as a solid gray ribbon. A stick representation of FAD is rendered in green, and acetoacetyl-CoA, a substrate analogue, is in purple. E368, the catalytic base, is also pictured in red. The carboxy terminus is marked, but the amino terminus is hidden from view.

This finding is reasonable when the effects of G185S and R147W substitutions on the predicted structure of human SCAD are considered (Figure 1). R147 is located on a β-barrel motif, which does not contribute to monomer interactions or directly to binding of FAD in the substrate-binding pocket. G185, in contrast, is predicted to be located near the opening of the substrate-binding pocket. While it is not likely to interact directly with the substrate, substitution of this residue with a serine would alter the hydrophobicity of the local environment. Similarly, neither substitution is likely to directly affect FAD binding. Rather, our data suggest that the G185S substitution has a greater effect than R147W on the change in conformation or electronic configuration in response to substrate binding, and results in more severe impairment of enzyme function. Our ability to evaluate this directly through monitoring the change in the tryptophan fluorescence signal upon substrate binding is limited due to the presence of the additional tryptophan residue in the

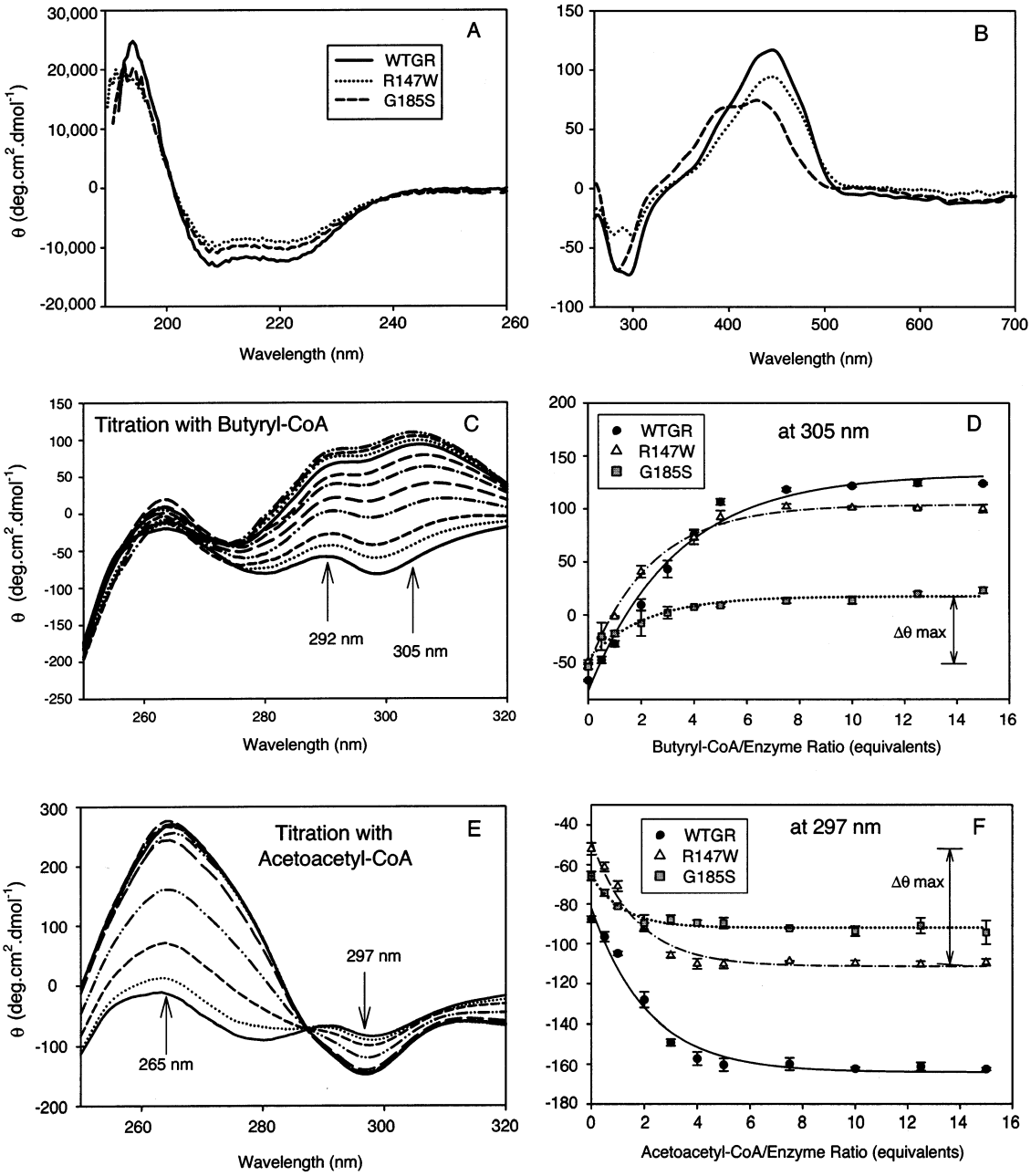

FIGURE 2: Circular dichroism spectra of SCADs with and without added substrate. (A) Far-UV CD spectra of WTGR (0.82 μM), R147W (0.58 μM), and G185S (0.72 μM). (B) Near-UV and visible CD spectra of WTGR and variant SCADs (5 μM final concentrations). (C) Near-UV CD spectra of WTGR titration with butyryl-CoA. The curve with the lowest molar ellipticity at 305 nm corresponds to no added substrate, and there is an increase in molar ellipticity at this wavelength with increasing butyryl-CoA concentration from 0 to 69.8 μM as in Materials and Methods. (D) Relationship between molar ellipticity and the substrate:enzyme ratio (equivalents) in the titration of WTGR, R147W, and G185S with butyryl-CoA at 305 nm. (E) Near-UV CD spectra of WTGR titration with acetoacetyl-CoA. The curve with the lowest molar ellipticity at 265 nm corresponds to no added acetoacetyl-CoA, and there is an increase in molar ellipticity at this wavelength with increasing acetoacetyl-CoA concentrations from 0 to 69.8 μM as in Materials and Methods. (F) Relationship between molar ellipticity and the substrate:enzyme ratio (equivalents) in the titration of WTGR, R147W, and G185S with acetoacetyl-CoA at 297 nm. The curves in panels D and F were fit by eq 1 with p value of <0.0001.

R147W variant. We therefore pursued additional spectrophotometric and near-UV wavelength CD analysis for this purpose.

Absorbance Spectroscopy of Purified Wild-Type and Variant SCAD Proteins. All ACDs show a characteristic spectral absorption pattern with maxima around wavelengths of 365 and 450 nm related to the noncovalently bound FAD coenzyme (*28*, *37*−*39*). When the enzyme is incubated with the butyryl-CoA substrate under anaerobic conditions, reduction of FAD occurs and decreases these absorbance maxima. At the same time, a new broad higher-wavelength maximum appears at ∼560 nm, reflecting establishment of the stable charge transfer enzyme−substrate intermediate between the highest occupied molecular orbital of the flavin and the lowest unoccupied molecular orbital of the polarized crotonyl-CoA product (*45*−*47*). In the reductive half-reaction model proposed by Thorpe et al. (*48*), six enzyme species exist at the equilibrium state: $EFAD_{ox}$, $EFAD_{red}$, $EFAD_{ox}$·C4CoA, $EFAD_{ox}$·CCoA, $EFAD_{red}$·C4CoA, and $EFAD_{red}$·CCoA. Three species containing FAD in reduced form

($EFAD_{red}$, $EFAD_{red}$•C4CoA, and $EFAD_{red}$•CCoA) are closely related to the specific absorbance change of FAD at 365 and 450 nm. Our results are consistent with the model. Wild-type SCAD and the variant SCADs showed similar changes in spectral profiles when incubated with butyryl-CoA with a decrease in the ~450 nm absorption maximum for all three enzymes. The characteristic FAD maximum at 444 nm, however, showed a slight red shift to 449 nm in the G185S variant. The G185S variant also showed slightly less reduction than the other enzymes at a 1:1 enzyme:substrate concentration ratio and excess substrate concentration, and required higher concentrations of substrate to reach half-maximal reduction (data not shown).

CD Spectroscopy of Purified Wild-Type and Variant SCAD Proteins. CD spectroscopy was used to study the conformation of enzyme−substrate complexes in the far-UV (*49*), near-UV (*50*, *51*), and visible CD spectra (wavelength ranges of 180−260, 250−320, and 320−700 nm, respectively). Figure 2 shows the average spectrum from triplicate measurements for each enzyme preparation. The far-UV CD spectra of wild-type SCAD, which predominantly reflects enzyme secondary structure, showed specific peaks at wavelengths of 194, 210, and 222 nm (Figure 2A). The wild-type enzyme coexpressed with GroEL/ES showed the strongest CD signal in the far-UV wavelength range. The near-UV and visible CD spectra (Figure 2B), largely determined by protein tertiary structure and the signals of the substrate-binding pocket containing FAD, respectively, exhibited minimal differences between wild-type and R147W variant enzymes, while the peaks for G185S were slightly larger with an altered shape.

The near-UV wavelength range is often used in CD spectroscopy to characterize the tertiary conformation change of protein structure through the CD signals at specific wavelengths for phenylalanine (255−270 nm), tyrosine and tryptophan (275−285 nm), and tryptophan (275−305 nm). Upon addition of butyryl-CoA to the purified SCADs, the variations in molar ellipticity of two specific peaks seen at 292 and 305 nm were fit by eq 1 and maximal changes in CD intensity ($\Delta\Theta_{max}$ values) were determined by eq 2. $\Delta\Theta_{max}$ values were 174 ± 8, 127 ± 4, and 54 ± 3 deg cm^2 dmol^{-1} at 292 nm and 205 ± 9, 152 ± 4, and 59 ± 5 deg cm^2 dmol^{-1} at 305 nm for WTGR, R147W, and G185S, respectively (Figure 2C,D), while major and minor $\Delta\Theta_{max}$ values were 338 ± 21, 268 ± 15, and 96 ± 4 deg cm^2 dmol^{-1} at 265 nm and -82 ± 5, -63 ± 4, and -26 ± 2 deg cm^2 dmol^{-1} at 297 nm with acetoacetyl-CoA, respectively (Figure 2E,F). The WTGR:R147W:G185S $\Delta\Theta_{max}$ ratio was approximately 1:0.75:0.3 at all observed wavelengths for the two substrates. Changes in tertiary structure in the enzyme upon butyryl-CoA substrate binding or nonproductive interaction with acetoacetyl-CoA (as shown by the calculated $\Delta\Theta_{max}$ values) reached maximal values in an identical order at these observed wavelengths: WT > R147W > G185S.

The visible CD spectrum of wild-type and R147W SCAD had one absorption maximum at 445 nm, while the G185S variant showed two broad peaks centered at 434 and 400 nm (Figure 2B). A decrease in the intensity of these peaks was seen upon addition of butyryl-CoA to the enzyme solution, while only minimal changes occurred upon addition of acetoacetyl-CoA or the reaction product crotonoyl-CoA (data not shown).

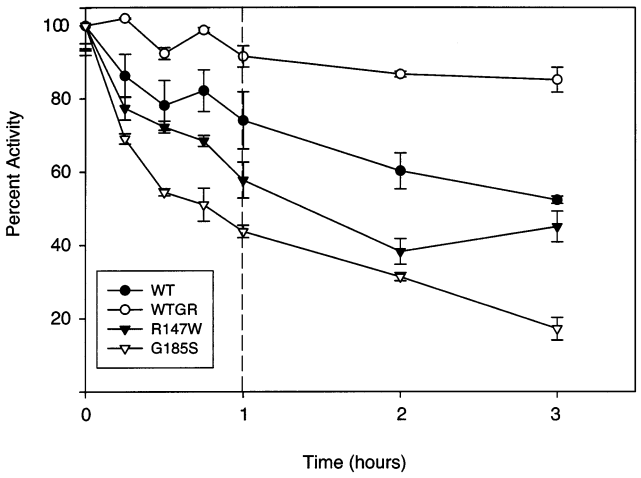

FIGURE 3: Temperature stability of purified wild-type and variant SCADs. A sample of the purified enzyme was incubated at 45 °C for the indicated time at pH 7.5 and the amount of remaining activity measured with the ferricenium hexafluorophosphate reduction assay. The percent of starting activity was calculated and graphed vs the time of incubation. Note that the time scale in the first hour (indicated with the dashed line) is expanded compared to the remaining time. Wild-type SCAD (WT), wild-type enzyme coexpressed with GroEL/ES (WTGR), and the two variants are shown as indicated in the legend.

To examine the microenvironment of Tyr and Trp residues of SCADs, secondary derivative UV spectra were collected for samples from the center of the tetramer peak after separation of each protein by SE-HPLC (*52*). The *r* values determined by the polarity of Tyr residues as well as by the relative ratio of Tyr to Trp as described previously (*52*) were 0.64, 0.59, 0.56, and 0.63 for WT, WTGR, R147W, and G185S, respectively. The reduced *r* value for the green wild-type enzyme when it is coexpressed with GroEL/ES implies that the folding effect caused by coexpression with GroEL/ES leads to the Tyr residues being less solvent exposed. The *r* value of the green G185S variant was higher than that of the green wild-type enzyme (WTGR), indicating that the microenvironment in the variant enzyme is more polar than that of the wild type, leading to a greater risk for denaturation. It is difficult to compare the R147W variant to the other enzymes due to the presence of the additional Trp residue. In total, our CD data suggest impairment in flexibility of the variant enzymes in assuming the tertiary structural changes induced by substrate binding.

Temperature and pH Stability of Wild-Type and Variant SCADs. Previous studies with crude extracts from mammalian cells overexpressing the variant SCADs suggested that they tolerate temperature extremes differently than the wild-type enzyme. To examine this further, activity studies of the purified enzymes were performed under different pH and temperature conditions. At temperatures of ≤37 °C, all of the enzymes were relatively stable after incubation for 5 h over a pH range of 6.0−8.0 in the presence of <3% glycerol (data not shown), but began to lose activity after incubation at higher and lower pHs. The response to prolonged incubation at a higher temperature at pH 7.5 was also more pronounced (45 °C, Figure 3). Under these conditions, the wild-type enzyme coexpressed with GroEL/ES lost only 15% of its activity. In contrast, the wild-type enzyme expressed without GroEL/ES and the R147W variant

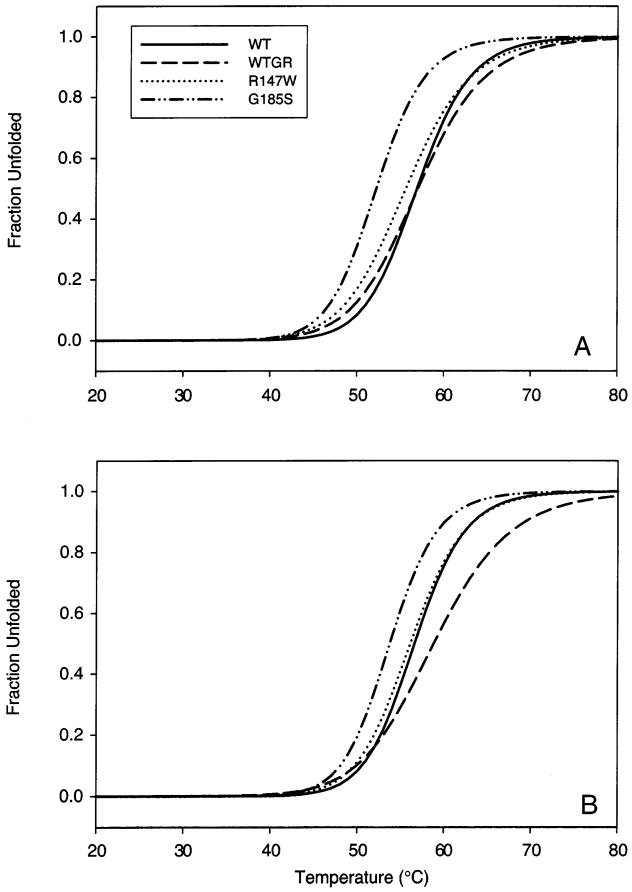

FIGURE 4: Thermal unfolding curves of purified wild-type and variant SCADs without (A) and with (B) added substrate as measured by the circular dichroism signal at 222 nm. The ratio of active subunits (estimated from the FAD content) to substrate was 1:1. Wild-type SCAD (WT), wild-type enzyme coexpressed with GroEL/ES (WTGR), and the two variants are shown in both panels as indicated in the legend.

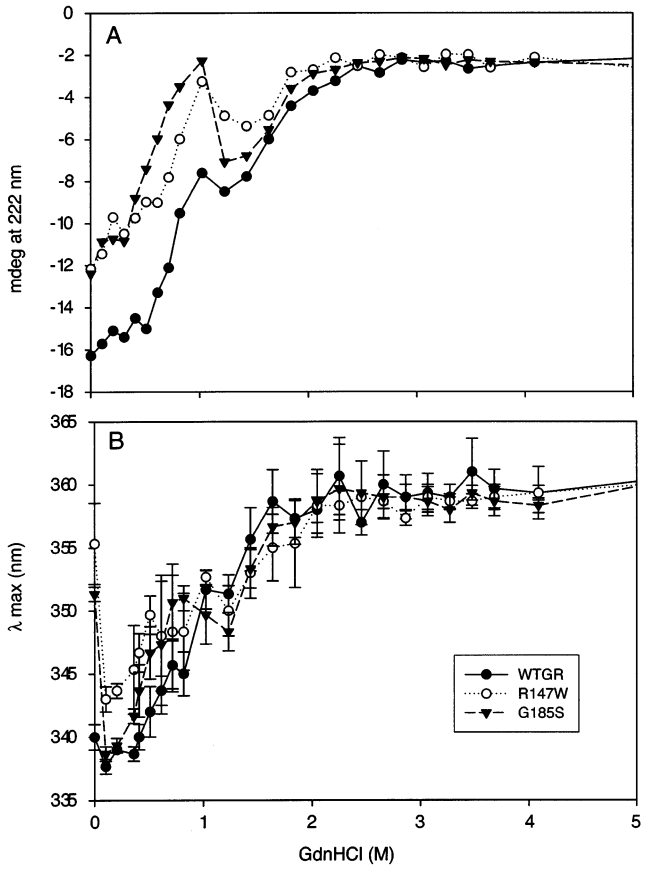

FIGURE 5: GdnHCl unfolding curves of purified wild-type and variant SCADs as measured by the circular dichroism signal at 222 nm (A) and the intrinsic fluorescence signal of tryptophan (B). The wild-type enzyme coexpressed with GroEL/ES (WTGR), and the two variants are shown as indicated in the legend.

dropped to approximately 50% of starting activity, while the G185S variant lost nearly 85% of its activity after 3 h.

Thermal Unfolding of Purified SCADs. To confirm that the decrease in enzymatic activity of the two variant enzymes at high temperatures was caused by decreased thermal stability of the tertiary and/or secondary enzyme structure, thermal unfolding of the SCADs was further investigated by CD and fluorescence spectroscopy (Figure 4) (*40*−*43*). The thermally induced unfolding for all of the SCADs was irreversible as determined by both fluorescence and CD methods. The temperature transition range was 45−70 °C for the wild-type enzyme coexpressed with GroEL/ES, 45−65 °C for the wild-type enzyme (without GroEL/ES coexpression) and R147W variant, and 45−60 °C for the G185S variant. The midpoint of the temperature transition (T_m), defined as the apparent midpoint of the thermal transition of the CD signal, was in the order of highest for the wild-type enzyme coexpressed with GroEL/ES (57 ± 0.3 °C), intermediate for R147W (55.6 ± 0.4 °C), and lowest for the G185S variant (52.2 ± 0.2 °C). Comparison of the extent of thermal unfolding of the purified SCADs as measured by fluorescence at an emission wavelength of 340 nm proved not to be useful because of a large red shift (20 nm) in the maximal Trp signal in the R147W variant.

GdnHCl Unfolding of Purified SCADs. Chemical-induced unfolding of the purified SCADs was studied with GdnHCl (*40*, *42*). The unfolding of enzyme secondary structure as indicated by the α-helix content was measured as a change in the far-UV CD signal at 222 nm, while the change in tertiary structures was measured by the tryptophan fluorescence spectra between 330 and 370 nm to follow λ_{max} with excitation at 295 nm (Figure 5A,B). In comparison to the wild-type enzyme expressed with or without GroEL/ES, the alteration of secondary structure of the two SCAD mutants proceeded at a higher rate even at room temperature and without the presence of GdnHCl (Figure 5A). The loss of secondary and tertiary structure is sequential, suggesting the presence of partially folded intermediates with substantial tertiary structure at GdnHCl concentrations between 0 and 0.1 M. The protein stabilization by GdnHCl is mediated by the interactions between the folding intermediates and GdnHCl either through an effect of GdnHCl on the structure of water (which requires a moderately high salt concentration) (*53*) or by electrostatic shielding (*54*). The latter may be pertinent at the low salt concentration used in these experiments, with an increase in Cl^- ion concentration in the enzyme test solution leading to an increased level of binding to positive charges on the protein molecule, and to formation of partially refolded intermediates (*55*). Complete denaturation of secondary and tertiary structure was seen at a GdnHCl concentration of 2 M. The GdnHCl concentrations causing 50% unfolding of tertiary structure (C_m) were 1.0 ± 0.1 and 0.98 ± 0.06 M for the wild-type enzyme with and without GroEL/ES, respectively.

CONCLUSION

Wild-type SCAD and SCADs corresponding to two common variant enzymes in the northern European population have been expressed in *E. coli* and purified. The G185S variant enzyme shows impairment of kinetic properties; however, structural modeling reveals the R147W and G185S substitutions are well outside of the substrate-binding pocket. Additional functional studies implicate a decreased flexibility in the tertiary conformation of the variant enzymes, leading to impairment in the establishment of the charge transfer substrate−enzyme intermediate complex as the cause for the catalytic dysfunction.

REFERENCES

1. Crane, F., and Beinert, H. (1955) *J. Biol. Chem. 218*, 717−731.
2. Ikeda, Y., Dabrowski, C., and Tanaka, K. (1983) *J. Biol. Chem. 258*, 1066−1076.
3. Ikeda, Y., Okamura-Ikeda, K., and Tanaka, K. (1985) *J. Biol. Chem. 260*, 1311−1325.
4. Ikeda, Y., and Tanaka, K. (1983) *J. Biol. Chem. 258*, 9477−9487.
5. Izai, K., Uchida, Y., Orii, T., Yamamoto, S., and Hashimoto, T. (1992) *J. Biol. Chem. 267*, 1027−1033.
6. Rozen, R., Vockley, J., Zhou, L., Milos, R., Willard, J., Fu, K., Vicanek, C., Low-Nang, L., Torban, E., and Fournier, B. (1994) *Genomics 24*, 280−287.
7. Willard, J., Vicanek, C., Battaile, K. P., Vanveldhoven, P. P., Fauq, A. H., Rozen, R., and Vockley, J. (1996) *Arch. Biochem. Biophys. 331*, 127−133.
8. Kim, J.-J., and Wu, J. (1988) *Proc. Natl. Acad. Sci. U.S.A. 84*, 6677−6681.
9. Kim, J. J. P., Wang, M., and Paschke, R. (1993) *Proc. Natl. Acad. Sci. U.S.A. 90*, 7523−7527.
10. Djordjevic, S., Pace, C. P., Stankovich, M. T., and Kim, J. J. P. (1995) *Biochemistry 34*, 2163−2171.
11. Tiffany, K. A., Roberts, D. L., Wang, M., Paschke, R., Mohsen, A. W. A., Vockley, J., and Kim, J. J. P. (1997) *Biochemistry 36*, 8455−8464.
12. Battaile, K., Molin-Case, J., Paschke, R., Wang, M., Bennett, D., Vockley, J., and Kim, J.-J. P. (2002) *J. Biol. Chem. 277*, 12200−12207.
13. Wanders, R. J. A., Vreken, P., Den Boer, M. E. J., Wijburg, F. A., Van Gennip, A. H., and IJlst, L. (1999) *J. Inherited Metab. Dis. 22*, 442−487.
14. Roe, C. R., and Ding, J. (2001) in *The Metabolic and Molecular Basis of Inherited Disease* (Scriver, C., Beaudet, A. L., Sly, W., and Valle, D., Eds.) pp 2297−2326, McGraw-Hill, New York.
15. Bhala, A., Willi, S. M., Rinaldo, P., Bennett, M. J., Schmidtsommerfeld, E., and Hale, D. E. (1995) *J. Pediatr. 126*, 910−915.
16. Corydon, M. J., Gregersen, N., Lehnert, W., Ribes, A., Rinaldo, P., Kmoch, S., Christensen, E., Kristensen, T. J., Andresen, B. S., Bross, P., Winter, V., Martinez, G., Neve, S., Jensen, T. G., Bolund, L., and Kolvraa, S. (1996) *Pediatr. Res. 39*, 1059−1066.
17. Dawson, D. B., Waber, L., Hale, D. E., and Bennett, M. J. (1995) *J. Pediatr. 126*, 69−71.
18. Niezen-Koning, K. E., Wanders, R., Nagel, G. T., Sewell, A. C., and Heymans, H. (1994) *Clin. Chim. Acta 229*, 99−106.
19. Tein, I., Haslam, R. H. A., Rhead, W. J., Bennett, M. J., Becker, L. E., and Vockley, J. (1999) *Neurology 52*, 366−372.
20. Vockley, J. (1994) *Mayo Clin. Proc. 69*, 249−257.
21. Gregersen, N., Winter, V. S., Corydon, M. J., Corydon, T. J., Rinaldo, P., Ribes, A., Martinez, G., Bennett, M. J., Vianey-Saban, C., Bhala, A., Hale, D. E., Lehnert, W., Kmoch, S., Roig, M., Riudor, E., Eiberg, H., Andresen, B. S., Bross, P., Bolund, L. A., and Kolvraa, S. (1998) *Hum. Mol. Genet. 7*, 619−627.
22. de Boer, H. A., and Kastelein, R. A. (1986) in *Maximizing gene expression* (Reznikoff, W., and Gold, L., Eds.) pp 225−285, Butterworth Publishers, Stoneham, MA.
23. Wynn, R., Davie, J., Cox, R., and Chuang, D. (1992) *J. Biol. Chem. 267*, 12400−12403.
24. Kubo, T., Mizobata, T., and Kawata, Y. (1993) *J. Biol. Chem. 268*, 19346−19351.
25. Grimm, R., Donaldson, G. K., Van der Vies, S. M., Schaefer, E., and Gatenby, A. A. (1993) *J. Biol. Chem. 268*, 5220−5226.
26. Ybarra, J., and Horowitz, P. M. (1995) *J. Biol. Chem. 270*, 22113−22115.
27. Tian, G., Vainberg, I. E., Tap, W. D., Lewis, S. A., and Cowan, N. J. (1995) *Nature 375*, 250−253.
28. Battaile, K., Mohsen, A.-W., and Vockley, J. (1996) *Biochemistry 35*, 15356−15363.
29. Mohsen, A.-W. A., and Vockley, J. (1995) *Biochemistry 34*, 10146−10152.
30. Mohsen, A. A., and Vockley, J. (1995) *Gene 160*, 263−267.
31. Wilson, C. M. (1983) in *Methods in Enzymology* (Hirs, C. H. W., and Timasheff, S. N., Eds.) pp 236−247, Academic Press, New York.
32. Shaw, L., and Engel, P. C. (1987) *Biochim. Biophys. Acta 919*, 171−174.
33. Williamson, G., and Engel, P. C. (1982) *Biochim. Biophys. Acta 706*, 245−248.
34. Williamson, G., Engel, P. C., Mizzer, J. P., Thorpe, C., and Massey, V. (1982) *J. Biol. Chem. 257*, 4314−4320.
35. Lehman, T. C., Hale, D. E., Bhala, A., and Thorpe, C. (1990) *Anal. Biochem. 186*, 280−284.
36. Mohsen, A.-W., Anderson, B., Volchenboum, S., Battaile, K., Tiffany, K., Roberts, D., Kim, J.-J., and Vockley, J. (1998) *Biochemistry 37*, 10325−10335.
37. Ikeda, Y., Okamura-Ikeda, K., and Tanaka, K. (1985) *Biochemistry 24*, 7192−7199.
38. Mohsen, A.-W. A., Aull, J. L., Payne, M. D., and Daron, H. H. (1995) *Biochemistry 34*, 1669−1677.
39. Dwyer, T., Rao, S., Goodman, S., and Frerman, F. (2000) *Biochemistry 39*, 11488−11499.
40. Kim, Y. S., Cape, S. P., Chi, E., Raffen, R., Wilkins-Stevens, P., Stevens, F. J., Manning, M. C., Randolph, T. W., Solomon, A., and Carpenter, J. F. (2001) *J. Biol. Chem. 276*, 1626−1633.
41. Kim, Y. S., Wall, J. S., Meyer, J., Murphy, C., Randolph, T. W., Manning, M. C., Solomon, A., and Carpenter, J. F. (2000) *J. Biol. Chem. 275*, 1570−1574.
42. Pace, C. N. (1986) *Methods Enzymol. 131*, 266−280.
43. Santoro, M. M., and Bolen, D. W. (1988) *Biochemistry 27*, 8603−8608.
44. Battaile, K. P., Kim, J.-J., and Vockley, J. (1995) *Am. J. Hum. Genet. 57*, A175.
45. Pellett, J. D., Becker, D. F., Saenger, A. K., Fuchs, J. A., and Stankovich, M. T. (2001) *Biochemistry 40*, 7720−7728.
46. Engel, P. C., and Massey, V. (1971) *Biochem. J. 125*, 889−902.
47. Nishina, Y., Sato, K., Hazekawa, I., and Shiga, K. (1995) *J. Biochem. 117*, 800−808.
48. Thorpe, C., Matthews, R. G., and Williams, C. H. (1979) *Biochemistry 18*, 331−337.
49. Sreerama, N., Manning, M., Powers, M., Zhang, J.-X., Goldenberg, D., and Woody, R. (1999) *Biochemistry 38*, 10814−10822.
50. Peyser, Y. M., Ajtai, K., Werber, M. M., Burghardt, T. P., and Muhlrad, A. (1997) *Biochemistry 36*, 5170−5178.
51. Strickland, E. H. (1974) *CRC Crit. Rev. Biochem. 2*, 113−175.
52. Ragone, R., Colonna, G., Balestrieri, C., Servillo, L., and Irace, G. (1984) *Biochemistry 23*, 1871−1875.
53. Goto, Y., Takahashi, N., and Fink, A. L. (1990) *Biochemistry 29*, 3480−3488.
54. Morjana, N. A., McKeone, B. J., and Gillbert, H. F. (1993) *Proc. Natl. Acad. Sci. U.S.A. 90*, 2107−2111.
55. Edwin, F., and Jagannadham, M. V. (2000) *Arch. Biochem. Biophys. 381*, 99−110.

BI026030R